

Observational Evidence of Mixed Rossby Gravity Waves at the Central Equatorial Indian Ocean

*P.M. Muraleedharan¹, S. Prasanna Kumar¹, K. Mohanakumar², S. Sijikumar³, K.U. Sivakumar¹, Teesha Mathew¹

¹National Institute of Oceanography, Goa, India

²Department of Atmospheric Sciences, Cochin University of Science and Technology, Kochi, India

³Space Physics Laboratory, Vikram Sarabhai Space Centre, Thiruvananthapuram, India

*Corresponding author: Tele/Fax : 91(0)832 2450285/91(0)832 2450608; Email: murali@nio.org

Abstract:

Six hourly soundings (GPS sonde) were carried out at the central equatorial Indian Ocean (80°–83° E) during 25th September to 10th October 2011 under the CINDY2011 (Cooperative Indian Ocean Experiment on Intra-seasonal variability in Year 2011) field campaign. One degree interval soundings were also taken along a meridional section at 83° E from 5° N to 5° S during 12 - 20 October 2011 to supplement the time series data. Relative humidity (RH) and meridional wind component exhibit downward propagation of air mass in bands of high and low RH associated with northerly and southerly winds respectively. Low (20-100 day) and high (2-10 day) frequency band pass filtered OLR data (NOAA interpolated OLR) revealed the presence of Madden and Julian Oscillation (MJO) with 20-40 day periodicity, and weak mixed Rossby Gravity (MRG) waves with 4-5 day periodicity. Eastward (westward) propagating MJO (MRG wave) with wave numbers 3 – 4 (4 – 5), amplitudes of anomaly 1.1 to 1.2 Wm⁻² (1.8 Wm⁻²) were observed. The asymmetric bifurcation of warm surface water by the subsurface cold water off Sumatra generate asymmetric convective regimes in the vicinity of the equator probably triggered convection with periodicity similar to MRG waves. The intermittent surface convection associated is believed to be responsible for the ascending moisture to the middle troposphere prior to the initiation of MJO. The moisture pumped to the middle troposphere makes the layer convectively more unstable leading to the state of deep convection, a situation conducive for the MJO initiation processes.

Key words: *Mixed Rossby Gravity Wave, Radiosonde data, Central Indian Ocean, Madden-Julian Oscillation, Latent heat flux*

Introduction

Wave-like motions with a period of approximately four to five days and a wavelength reaching to the order of 9000 km, with a structure similar to that of the mixed Rossby-gravity (MRG) waves are a prominent characteristic of the tropical atmospheric circulation (Matsuno 1966). Observational evidence of similar motions in the equatorial region was reported by Yanai and Maruyama (1966) and Maruyama (1967) who noticed fluctuations in the meridional wind of the stratosphere, exhibiting comparable periodicity. Zangvil and Yanai (1981) observed that the cloud covering the tropics had the same spectral peaks in terms of wave number and frequency, thereby resembling the MRG wave and suggesting a strong coupling between the waves and the moist convection. Several numerical modelling studies have highlighted both mid-latitude forcing and interaction with cumulus convection as essential for exciting Yanai waves – often referred to as MRG waves (Hayashi 1974; Hayashi and Golder 1978). Hayashi and Golder (1978) also showed that Kelvin and MRG waves could be generated through latent heat release even in the absence of mid-latitude disturbances. Observational evidence indicated the role of the mid-latitude disturbances for the excitation of MRG waves in the equatorial troposphere (Magaña and Yanai 1995). MRG waves could also be excited by a non-linear mechanism associated with the internal response of the atmosphere to the heat sources coupled with the typical tropical convective activity (Raupp and Silva Dias 2005). Asymmetric lateral forcing from the mid-latitudes was proposed theoretically by Mak (1969) and was later given support observationally by Zangvil and Yanai (1980).

It had also been documented that the high frequency Rossby, Kelvin and MRG waves propagate vertically and that they were most often observed in the stratosphere-troposphere interface (Wheeler et al. 2000; Mohanakumar 2008). These waves originated from the lower troposphere where they were forced to propagate vertically by topographic forcing or land-sea diabatic heating differences. The convectively coupled MRG wave appeared to be next in importance to the equatorial Rossby wave (Wheeler and Kiladis 1999). Many have attempted to study the process of the coupling of convection with MRG waves around the region of the dateline (Zangvil 1975a; Zangvil and Yanai 1981; Liebmann and Hendon 1990; Hendon and Liebmann 1991; Takayabu and Nitta 1993; Dunkerton and Baldwin 1995). These studies have also emphasized the distinction between the convectively coupled MRG waves and the tropical depression-type disturbances, with the latter having a similar frequency, but often more confined to the western Pacific. Hendon and Liebmann (1991) documented that the waves generated in this region were due to the unique meridional sea surface temperature (SST) distribution.

Hendon and Liebmann (1991) showed that the MRG waves were not only best defined during the boreal fall season, but they dominated the spectra of anti-symmetric convection and lower tropospheric equatorial meridional winds near the date line. They further hypothesized that the dramatic localization of convectively coupled MRG waves to the central Pacific during the fall was due to the unique distribution of SST in the Pacific. During the fall, a well-defined equatorial minimum in the SST existed from the South American coast to about 160° E, leaving warm water on either side of the equator. In this region, a well-defined double Inter-tropical Convergence Zone (ITCZ) existed, where the convectively coupled MRG waves originated. According to Hendon and Liebmann (1991), the distributions of 4-5 day OLR and meridional wind variance and their coherence indicative of MRG wave activity clearly coincide with the region of the split in the ITCZ and SST. They further concluded that the generation of convectively coupled MRG waves depended more on local conditions that encourage anti-symmetric convection to develop, rather than remote forcing. All the processes act either to inhibit symmetric convection or to directly force asymmetric disturbances as highlighted by Itoh and Ghil (1988).

An organized field campaign was conducted under the Mirai Indian Ocean Cruise for the Study of the MJO-Convection Onset (MISMO) program over the central equatorial Indian Ocean during October to December 2006 (Yoneyama et al. 2008a). MISMO encountered the initiation of a weak MJO and noteworthy three- to four-day cycles in moisture and meridional wind at 500-400 hPa level. The horizontal wind structure suggested that the three- to four-day period variations were associated with the MRG wave (Yasunaga et al. 2010). Nasuno et al. (2007) emphasized the importance of the MRG wave disturbances during an MJO event using a numerical model.

In this paper, we report the observational evidence of downward (upward) propagation characteristics in the upper half (lower half) of the troposphere in both wind and humidity fields more or less resembling MRG wave periodicity. Details of the data and methodology used are described in the following section. The results are discussed in the subsequent section. The summary of the investigation is given in the last section of this paper

Data and methodology

As a part of the Cooperative Indian Ocean Experiment on Intra-seasonal variability in Year 2011 (CINDY2011), a field campaign with participation of 16 countries was conducted, in which we collected, from the central equatorial Indian Ocean (80°–83° E), six hourly continuous sounding data observations and a longitudinal section using the DigiCORA III MW31 Vaisala system during the 289th cruise of the ORV Sagar Kanya from 25th September to 20th October 2011. Sixteen-day time series of the vertical

profiles (12 km) were collected between 80° E and 83° E of the equator and a meridional section from 5° N to 5° S, centred at 83° E with 1° latitude interval soundings were also taken during the campaign. All the Vaisala RS92 radiosondes were calibrated and procured six months prior to the campaign. The total profile height (12km) is divided into three layers of equal thickness and categorised as lower (0- 4 km), middle (4 – 8 km) and upper (8 – 12 km) troposphere to make the discussion meaningful.

The science rationale and hypotheses, experimental design and operation, data collection and preliminary results of the field campaign were summarized by Yoneyama et al. (2013). All surface meteorological observations were collected at three-hourly intervals using the surface meteorological kit supplied by *Dynalab*, India. Kestrel 4500 pocket weather tracker was used to measure surface relative humidity and *Theodor Friedrichs* (type no. 5020) barometer was used for recording sea level pressure. TROPFLUX reanalysis data (Praveen Kumar et al., 2012) was used for mapping SST anomaly in the Indian-Pacific sector to resolve the evolution of *La Niña* in the Pacific in 2011. The anomaly was calculated by removing the climatological mean (1979 – 2012) from the respective monthly values. The dipole mode index (DMI) during October from 2001 to 2011 is taken from the weekly values derived from NOAA OI SST version 2 given at JAMSTEC site (http://www.jamstec.go.jp/frcgc/research/d1/iod/HTML/Dipole_Mode_Index.html). NOAA interpolated OLR data (Liebmann and Smith 1996) over the Indo-Pacific region were used to bring out the characteristics of MJO (20-100 day band pass filtered) and MRG (2-10 day band pass filtered) waves by examining symmetric and asymmetric components of the background removed wave number-frequency diagram during the period of observation. The near-surface warming caused by the ship structure introduced certain bias in the radiosonde data that were corrected following Yoneyama et al. (2002). The dry bias correction scheme had also been developed by Yoneyama et al. (2008b) to correct the radio sonde derived RH for daytime solar heating effects.

Results and discussion

The evolution of *La Niña* in 2011 started with an extreme event in January when the sea surface temperature (SST) anomaly almost reached -2° C in the *Niño 3.4* region and then subsided progressively to enter the warming phase in July 2011 (Figure 1). The re-emergence of a moderate cold phase followed immediately to establish an SST anomaly close to -1° C, which incidentally coincided with the moderate positive phase of the Indian Ocean Dipole (IOD) that peaked in October 2011. During this period, the negative SST anomalies offshore of Sumatra were less than 1° C, while the positive SST anomalies in the western Indian Ocean were close to 1° C (Gottschalck et al. 2013). As the negative SST

anomalies offshore of Sumatra quickly faded away, the positive phase of the IOD was practically terminated, except for a few scattered positive SST anomalies that persisted until December 2011. During a positive IOD (as in October 2011) event the warm water at the eastern equatorial Indian Ocean bifurcate pole ward to accommodate up welled cold water as shown in Figure 2a. By examining similar cases for the last ten years prior to 2011, three boxes (Box1 82-100E, 0-10N; Box2 82-100E, 0-15S; Box 3 80-100E, 15-25S) have been demarcated in the eastern equatorial Indian Ocean to visualise the dynamics in the inter-annual scale. The average temperature anomaly during October is then calculated at each box and the amplitude of variation is represented through bar diagram from 2001 to 2011 superimposed by October dipole mode index (DMI) (Figure. 2b). The years in the X-axis are not to scale as SST anomalies and DMI's are representing the month October when the Indian Ocean Dipole is in its peak. Positive DMI values during 2002, 2006, 2007, 2008 and 2011 closely coincided with the bifurcation of warm water (boxes 1 & 3) sandwiching relatively cooler up welled water (box 2). The strongest event in 2006 is associated with coolest water sandwiched between warmer water. The variation in amplitude, especially the absence (or slight positive values) of cooler anomaly, in 2001, 2008 and 2011 is associated with the averaging of anomalies in respective boxes. On the other hand the negative DMI values did not indicate any presence of cool water. Time series of six hourly observations of temperature (with superimposed lapse rate computed at every 100 m), relative humidity, and zonal and meridional wind components with height from the surface to 12 km altitude for the entire observational period are illustrated in Figure 3. Although the temperature distribution does not indicate any specific pattern, the intermittent patches of low lapse rate in the lower and middle troposphere indicated the presence of inversions prescribing relatively stable lower half, leaving a strip of unstable boundary layer beneath (Figure 3a). Patches of dry and humid air progressively descending to the lower troposphere were noticed in the RH time series with four to five days periodicity (see Figure 3b), especially above the 4 km height. An ascending feature of high and low humidity patches from the boundary layer was also discernible in the lower troposphere, with the same periodicity but at a lesser rate (Figure 3b). It was worthwhile to have a closer look at the six hourly time series of the zonal and meridional components of the wind profile above the central equatorial Indian Ocean. The upper (easterly flow) and lower (westerly flow) branches of the Walker circulation were noticed in the zonal wind component (Figure 3c). The meridional components of the wind speed also indicated the descending characteristics of both the northerly and southerly components, with similar periodicities (four to five days) above 4 km height with some signs of upward propagation below it (Figure 3d). Interestingly, four to five days periodicity was observed in the RH, as well as in the zonal and

meridional wind fields and it appeared to be embedded in the two branches of the Walker cell as seen from the zonal component of the wind field.

The wavelet analysis of the six hourly observations of temperature, RH and wind speeds in the lower (1.5 km), middle (6km) and upper (11km) troposphere over the observational site further confirmed the presence of the four to five day wave in the near-equatorial atmosphere (see Figure 4). Although the temperatures at the lower and upper troposphere indicated a well-defined periodicity, the variability at the middle troposphere displayed a mixture of four to five days (significant) and eight days (less significant) periodicities (Figure 4a-c). Strong 4-5 day periodicity in RH was noticed throughout the period of observation in the lower troposphere and it is less significant, except for a few days in the middle layer (Figure 4d and e). However, a prominent eight-day periodicity was also noticed at the higher troposphere during the entire time series (see Figure 4f). The zonal wind speed again followed more or less the same pattern of the RH, indicating that the shape was grossly reoriented in the upper troposphere (Figure 4g-i). However, a significant four- to five-day periodicity was noticed in the meridional wind speed in the middle troposphere while it deteriorated to statistically insignificant levels at the lower and upper troposphere (Fig. 4j-l). This is in contrast to the observation of Yasunaga *et al.* (2010) the largest amplitude (3-4 days) at 500-400 hPa in the year 2006 close to our location,

The time series of the zonal wind did not display any propagation characteristics as seen in the meridional wind pattern and RH. This peculiar nature indicates that the Kelvin waves seem to be less prominent or absent in the vicinity of the area of investigation. These types of waves were often propagated symmetrically to the equator and made noticeable undulations in the zonal field (Holton, 2004). The nature of propagation and the periodicity of the observed atmospheric parameters resemble those of the Mixed Rossby Gravity (MRG) waves and it appeared to coexist with the split in ITCZ noticed in 2006 and 2011. As the MRG waves are often found asymmetric to the equator, their characteristics are most visible only in the meridional component rather than in the zonal field. The shift in periodicity of MRG waves from 15 to 5 days is quantitatively consistent with the Doppler shift by horizontal shear as shown through model analysis by Hayashi and Golder (1978) and through observational analysis by Zangvil (1975). A detailed analysis indicated that most of the characteristics that were documented for the typical MRG waves (Mohankumar 2008) matched with the characteristics noticed in the observed data.

The meridional sections of temperature (superimposed with lapse rate), RH, zonal and meridional wind components from 5° N to 5° S at 83° E during mid-October are illustrated as contour plots in Figure 5.

The low lapse rate patches, which roughly follow the temperature contour in the lower half, denote a relatively stable meridional layer (Figure 5a). The dry air appeared to descend from the top to the middle troposphere as depicted in Figure 5b by virtue of its increased buoyancy in comparison with the adjoining lighter moist air mass. The zonal component of the wind, as displayed in Figure 5c, captured the two branches of the Walker circulation in the equator. The vertical migration of both the northerly and southerly components of the wind speed is clearly visible in the meridional section (Figure 5d). It is believed to be associated with the synoptic scale low pressure systems and associated convective activity over the central equatorial Indian Ocean during the CINDY-DYNAMO-2011 period (October 2011 to March 2013) as reported by Judt and Chen (2014). Four intra-seasonal and eastward propagating large-scale convective events occurred over the tropical IO in late October, late November, late December, and March, respectively (Yoneyama et al., 2013). Out of four, the October and November event barely reached the Pacific due the prevailing LaNina condition. However, the identity of these events has been established through either the real-time multivariate MJO index (Wheeler and Hendon, 2004) or MJO spectral filtering (Wheeler and Weickmann, 2001) applied to OLR. Yoneyama et al., (2013) called these events as MJO1 and MJO2 for convenience. The synoptic scale low pressure systems observed during late September and early October can be attributed to the initiation of MJO-1 that subsequently triggered MJO-2. A significant portion of the convective activity during MJO initiation was associated with Rossby- or mixed Rossby-gravity wave-like synoptic-scale systems during DYNAMO as shown by Kerns and Chen (2014) and Zuluaga and Houze (2013). The humidity and wind maps at 400 hPa during the first half of the observation period (figure not shown) indicate the migration of extra tropical air mass to the equator from both north and south, carrying humid and dry air mass respectively. The dry southerly air mass appears to descend to the boundary layer at the equator (Figure 5d) while the ascending humid air from either side of the equator (Figures 2a & 5d) was associated with the asymmetric warming (convection) zones due to asymmetric split in ITCZ, bifurcated by the intruding cold water during a Positive IOD event.

Several studies in the past have noted that moistening of the equatorial region is a necessary prerequisite to MJO initiation (see Yoneyama et al. 2013). Without sufficient moisture there can be no widespread deep convection and no MJO. When deep convection is concentrated in the ITCZ off the equator, there is likely to be some large-scale subsidence induced over the equator, which is unfavorable for equatorial convection. A similar situation occurred at the central Indian Ocean prior to the initiation of MJO-2 during CINDY-DYNAMO 2011 (Kerns and Chen, 2014). We have noticed similar double ITCZ at the eastern equatorial Indian Ocean due to the pole-ward bifurcation of warm air to accommodate IOD

forced cold up welled water (Figure 2a) and descending (subsidence) dry air at the equator (Figure 5b) during late September and early October 2011 prior to the MJO-1. The asymmetric convective activity associated with the double ITCZ could be associated with the MRG wave like synoptic-scale systems during this period as explained by Kerns and Chen (2014).

MJO and MRG waves are associated with deep convection. They create considerable changes in the amount of Outgoing Long wave Radiation (OLR) and hence OLR is considered as a reasonable proxy for convection. To identify the tropical waves, the OLR data was filtered following Wheeler and Weickmann (2001). The daily OLR anomalies were calculated by subtracting the 61 days (1st September to 31st October 2011) mean individual grid value. Equatorial symmetry is not considered. The Hovmuller (longitude-time) diagram of the 20-100 day band pass filtered daily OLR data averaged over latitudes 10° S and 5° N for the period from 1st of September 2011 to 31st of October 2011 is shown in Figure 6. In the 40° E to 100° E part of the near equatorial region, the presence of 30-40 day Madden Julian Oscillation (MJO) is clearly noted in the OLR data. It has been noted that the majority of the spectral peaks of tropical convection is found in the range of planetary to synoptic scales, and from intraseasonal timescales down to a period of 1.25 days (Wheeler and Kiladis, 1999). According to them, the Equatorial Kelvin (EK) waves in terms of convective variance stand close to MJO followed by Equatorial Rossby (ER) waves. In terms of amount of variance explained globally, the convectively coupled MRG wave appears to be the next in importance after the ER wave. For getting further insight for detecting the presence of MRG waves in OLR data, the background removed wave number frequency diagram for anti-symmetric wave type in the OLR data averaged over 10° S - 10° N are presented with the dispersion curve superimposed in figure 7. The presence of westward propagating asymmetric waves with the period of ~4-5 days, having wave number of 2-4 is also detected. Amplitude of OLR anomalies is of the order of 1.8 Wm⁻². Similar 2-6 days periodicity was noticed in the eleven episodes of rainfall in the vicinity of the CINDY/DYNAMO quadrilateral (Zuluaga and Houze, 2013). They speculate that this 2-6 days modulation is due to westward propagating synoptic-scale equatorial waves. Significant share of power in the anti-symmetric component attributes to MRG wave for wave numbers 2-4 and the same is true for MJO in the symmetric component. Extra-tropical wave energy is another possible source of MRG disturbances (Magana and Yanai, 1995).

The latent heat and sensible heat fluxes (LHF and SHF) computed from the COARE 3.0 bulk algorithm (Fairall et al., 2003) at every three-hour interval, using the surface meteorological data collected onboard, displayed similar intraseasonal signals with four to five day periodicity (Figure 8). The subsiding dry air at the equator often promotes intense evaporation due to humidity gradient and their effect is more

evident on either side of the equator. At the equator the descending dry air masks the convection and displayed weak ascending signature (Figure 3b & d). The intermittent shooting of the LHF and SHF on either side of the equator with the above periodicity pumped the moisture into the lower troposphere as seen in the time series profile (Figure 3b). Possibly this ascending humid air mass from lower troposphere can provide enough latent heat to trigger MRG wave in the upper troposphere as pointed out by Hayashi and Golder (1978). Convectively coupled MRG waves displayed large amplitudes with four to five day periodicity only in a limited region of the India-Pacific sector near the dateline and only during the boreal fall (Hendon and Liebmann 1991). Anti-symmetric convection was most coherent with the winds in the lower troposphere, but significant correlation was seen throughout the troposphere. The distinct autumnal peak of four to five days in the meridional wind component at 850 hPa at the equator and near the dateline was first noted by Julian (1971). The penetration of cold water from the South American coast to about 160° E during fall diverges the warm surface water (>28° C) to promote a split in the ITCZ. The distribution of the four- to five-day OLR and meridional wind variance and their coherence, indicative of MRG wave activity, clearly coincided with the region of the split in the ITCZ and SST (Hendon and Liebmann 1991). The presence of the MRG waves in the central equatorial Indian Ocean during autumn was reconfirmed by Yasunaga *et al.* (2010) through their well-planned field experiment onboard the *RV Mirai* in 2006. Incidentally, the year 2006 witnessed a strong positive dipole, wherein a cold tongue of up-welled water bifurcated the warm surface water into the meridional regime, supporting the formation of a double ITCZ. This could be linked to the presence of MRG wave in the boundary layer. The CINDY field campaign in 2011 also witnessed the emergence of a strong positive dipole event in October (boreal fall). Incidentally, it is worthwhile to highlight a similar split in SST at the eastern equatorial Indian Ocean during October 2011 (see Figure. 2a) by the cold tongue of up-welled water penetrating westward, splitting the surface warm water which could possibly demonstrate a split in ITCZ. The associated dynamics provided enough evidence for the asymmetric MRG wave activity at the boundary layer.

The observation of downward propagating MRG waves with four to five day periodicity interacted with the air-sea exchange processes of the boundary layer, causing intermittent overshooting of convection with similar periodicity in the boundary layer. Such injection of moisture into the lower troposphere, as seen in the time series (Figure 5b), could make the layer convectively unstable, eventually leading to deep convection. Similar processes have been explained by Li (2014) in the central Indian Ocean with different dynamics. The general hypothesis is that MJO initiation arises from the circumnavigation of a preceding MJO event. According to Li (2014), the forcing from the upstream (west of initiation region)

holds a key for triggering new convection over the western Indian Ocean. In this paper, we report the occurrence of similar high frequency waves in the central equatorial Indian Ocean and its possible association with the more complicated MJO activity during this period. We have not excluded the possibility of the coincidence of the MRG wave activity prior to the MJO onset during the CINDY period. We were left with no clue as to whether there would be similar occurrences in future MJO initiation processes as various climatic modes interact differently in this part of the ocean at various time scales.

Summary

Six hourly time series of high resolution radiosonde profiles in the central equatorial Indian Ocean lasting for sixteen days—from the 25th September 2011—over the equator, and one degree interval soundings from 5° N to 5° S at 83° E (12th to 20th of October) were analysed. The time series of humidity and meridional wind components displayed well-defined propagation characteristics of low (southerly) and high (northerly) humidity (wind component) bands from the upper to the middle troposphere. Similarly, upward propagations were also detected in the lower troposphere with less intensity on both the RH and the meridional wind. The wavelet analysis of the time series further confirmed the presence of four to five days wave activity. The characteristics of the wave detected in the time series resembled that of the MRG wave that was asymmetric to the equator.

The MJO filtered OLR data averaged over latitudes 10° S and 5° N during the period of observation exhibited the presence of 30-40 day MJO activity. Both westward and eastward moving periodicities in the wave number range 2-4 were discernible in the lowest frequency bands. The MRG filtered OLR, on the other hand, exhibited weak presence of westward propagating asymmetric waves with the period of ~4-5 days, having wave number of 2-4. The amplitude of the OLR anomalies is of the order of 1.8 Wm⁻². The vertical migration of the northerly and the southerly wind associated with humid and dry air masses, respectively, was displayed in the meridional section. Bifurcation of warm water was noticed in the central Indian Ocean during fall inter-monsoon season on either side of the equator separated by a cold tongue of up-welled water off Sumatra, a feature normally associated with positive dipole phase (Figure 2). This anomalous warming pattern induced asymmetric convective regimes. The descending dry air inhibits convection at the equator thereby leaving subdued propagation signs in the RH and wind time series. The enhanced convection on either side of the equator in alignment with the asymmetric warming pattern trigger MRG type disturbance. It is, therefore, worth emphasising that the bifurcation of warm water in response to the prevailing positive dipole situation appeared to trigger the

MRG wave activity in the central equatorial Indian Ocean. The intermittent enhancement of convection in the boundary layer injected moisture into the lower troposphere and transported it upward as seen in the time series. Due to the intermittent injection of moisture from the boundary layer, the lower troposphere became convectively more unstable, eventually leading to deep convection. It had been documented that the intra-seasonal ascending motion of humid air mass appeared in the lower troposphere 10 days prior to the convection initiation that led to the MJO-1 activity in October 2011. The MRG wave activity observed in our campaign however falls roughly two weeks prior to the initiation of the MJO-1. It appeared that the MJO initiation could be linked to the MRG wave activity. Alternatively, the MRG waves could have facilitated MJO amplification and/or the MJO circulation state that favoured MJO organization could also have generated an environment favourable for the MRG wave packet. The possibility of a lagged occurrence of the MRG wave and the MJO could be examined by extending the field campaign from an intra-seasonal to an inter-annual time scale by incorporating the natural combinations of various climate modes and their selective roles on the MRG wave-MJO activity.

Acknowledgement:

*The authors are thankful to the Director, CSIR-NIO, Goa, for providing support and facilities. We thank the Department of Science and Technology, Government of India, for financial support. The authors also thank the NOAA/OAR/ESRL PSD, Boulder, Colorado, USA, for the interpolated OLR data available at the web site <http://www.esrl.noaa.gov/psd/>. Our sincere thanks are also due to the organizers of CINDY/DYNAMO field campaign for coordinating various field measurements. This is NIO contribution number *****.*

References

- Carlos F, Raupp M, Dias PLS (2005) Excitation mechanism of mixed Rossby–Gravity waves in the equatorial atmosphere: Role of the nonlinear interactions among equatorial waves. *J Atmos Sci* 62: 1446-1462.
- Charney JG, Drazin PG, (1961) Propagation of planetary-scale disturbances from the lower into the upper atmosphere. *J Geophys Res* 66: 83–109.
- Dunkerton TJ, Baldwin MP, (1995) Observation of 3–6 day meridional wind oscillations over the tropical Pacific, 1973–1992: Horizontal structure and propagation. *J Atmos Sci* 52: 1585–1601.
- Fairall CW, Bradley ER, Hare JE, Grachev AA, Edson JB (2003) Bulk parameterization of air-sea fluxes: Updates and verification for the COARE algorithm. *J Clim* 16: 571-591.

- Gottschalck J, Roundy PE, Schreck III CJ, Vintzileos A, Zhang C, (2013) Large-scale atmospheric and oceanic conditions during the 2011-2012 DYNAMO Field Campaign. *Mon Wea Rev* 141: 4173 – 4196. Doi: <http://dx.doi.org/10.1175/MWR-D-13-00022.1>
- Hayashi Y (1974) Spectral analysis of tropical disturbances appearing in a GFDL general circulation model. *J Atmos Sci* 31: 180–218.
- Hayashi Y, Golder DG (1978) The generation of equatorial transient planetary waves: Control Experiments with a GFDL General Circulation Model. *J Atmos Sci* 35:2068–2082.
- Hendon HH, Liebmann B (1991) The Structure and annual variation of antisymmetric fluctuations of tropical convection and their association with Rossby–gravity waves. *J Atmos Sci* 48: 2127–2140.
- Holton JR (1980) Wave propagation and transport in the middle atmosphere. *Phil Tran Roy Soc Lon Math Phys Sci* 296:73-85.
- Holton JR (2004) *An Introduction to Dynamic Meteorology - Fourth edition*. International geophysics series. ISSN 0074-6142 Elsevier Academic Press, pp535.
- Itoh H, Ghil M (1988) The Generation Mechanism of Mixed Rossby-Gravity Waves in the Equatorial Troposphere. *J Atmos Sci* 45:585 – 604.
- Judt F, Chen SS, (2014) An explosive convective cloud system and its environmental conditions in MJO initiation observed during DYNAMO. *J Geophys Res (Atmos.)* 119, doi:10.1002/2013JD021048.
- Julian P (1971) Some aspects of variance spectra of synoptic scale tropospheric wind components in midlatitudes and in the tropics. *Mon Wea Rev* 99: 954-965.
- Kerns BW, Chen SS, (2014) Equatorial dry air intrusion and related synoptic variability in MJO initiation during DYNAMO. *Mon Wea Rev* 142:1326–1343. doi:10.1175/MWR-D-13-00159.1.
- Li Tim (2014) Recent advance in understanding the dynamics of the Madden-Julian oscillation. *J Meteor Res* 28: 001 – 033. Doi: 10.1007/s13351-014-3087-6.
- Liebmann B, Hendon HH (1990) Synoptic-scale disturbances near the equator. *J Atmos Sci* 47:1463–1479.
- Liebmann B, Smith CA (1996) Description of a Complete (Interpolated) Outgoing Long wave Radiation Dataset. *Bull. American Met Soc* 77:1275-1277.
- Magana V, Yanai M (1995) Mixed Rossby-gravity waves triggered by lateral forcing. *J Atmos Sci* 52:1473–1486.
- Maruyama T (1967) Large-scale disturbances in the equatorial lower stratosphere. *J Meteor Soc Japan* 45:391–408.
- Mak MK (1969) Laterally driven stochastic motions in the tropics. *J Atmos Sci* 26:4-64.
- Matsuno T (1966) Quasi-geostrophic motions in the equatorial area. *J Meteor Soc Japan* 44:25–43.
- Mohanakumar K (2008) *Stratosphere Troposphere Interactions: An Introduction*. Springer pp416.
- Nasuno T, Tomita H, Iga S, Miura H, Satoh M (2007) Multi scale organization of convection simulated with explicit cloud processes on an aqua planet. *J Atmos Sci* 64:1902–1921.

- Praveen Kumar B, Vialard J, Lengaigne M, Murty VSN, McPaden MJ (2012) TropFlux wind stresses over the tropical oceans: evaluation and comparison with other products. *Clim Dyn* 38:1521 – 1543. DOI 10.1007/s00382-012-1455-4
- Saji NH, Goswami BN, Vinayachandran PN, Yamagata T (1999) A dipole mode in the tropical Indian Ocean. *Nature*, 401: 360-363.
- Takayabu YN, Nitta T (1993) 3–5 day period disturbances coupled with convection over the tropical Pacific Ocean. *J Meteor Soc Japan* 71:221–246.
- Wheeler M, Hendon HH (2004) An all-season real-time multivariate MJO index: Development of an index for monitoring and prediction. *Mon Wea Rev* 132: 1917-1932.
- Wheeler M, Kiladis GN, Webster PJ (2000) Large-scale dynamical fields associated with convectively coupled equatorial waves. *J Atmos Sci* 57: 613-640.
- Wheeler, M, Weickmann KM (2001) Real-time monitoring and prediction of modes of coherent synoptic to intraseasonal tropical variability. *Mon Wea Rev* **129**: 2677-2694.
- Yasunaga K, Yoneyama K, Moteki Q, Fujita M, Takayabu YN, Suzuki J, Ushiyama T, Mapes B (2010) Characteristics of 3–4- and 6–8 day period disturbances observed over the tropical Indian Ocean. *Mon Wea Rev* 138:4158 – 4174.
- Yanai M, Maruyama T (1966) Stratospheric wave disturbances propagating over the equatorial Pacific. *J Meteor Soc Japan* 44:291–294.
- Yoneyama K, Hanyu M, Sueyoshi S, Yoshiura F, Katsumata M (2002) Radiosonde observation from the ship in the tropical region. *JAMSTEC. CR45*: 31-39.
- Yoneyama K, Masumoto Y, Kuroda Y, Katsumata M, Mizuno K, Takayabu YN, Yoshizaki M, Shareef A, Fujiyoshi Y, Mc Phaden MJ, Murty VSN, Shiroyaka R, Yasunaga K, Yamada H, Sato N, Ushiyama T, Moteki Q, Seiki A, Jujita M, Ando K, Hase H, Ueki I, Horii T, Yokoyama C, Miyakawa T (2008a) MISMO field experiment in the equatorial Indian Ocean. *Bull Amer Meteor Soc* 89:1889–1903.
- Yoneyama K, Fujita M, Sato N, Fujiwara M, Inai Y, Hasebe F (2008b) Correction for radiation dry bias found in RS92 radiosonde data during the MISMO field experiment. *SOLA*. 4:13-16.
- Yoneyama K, Zhang C, Long CN (2013) Tracking pulses of the Madden-Julian Oscillation. *Bull American Met Soc* 94:1871–1891,doi:10.1175/BAMS-D-12-00157.1.
- Zangvil A (1975a) Temporal and spatial behavior of large-scale disturbances in tropical cloudiness deduced from satellite brightness data. *Mon Wea Rev* 103: 904–920.
- Zangvil A (1975b) Upper tropospheric waves in the tropics and their association with clouds in the wavenumber-frequency domain. Ph.D. thesis, Meteor. Pap. Nos. 13 and 14, University of California, Los Angeles, pp131.
- Zangvil A, Yanai M (1980) Upper tropospheric waves in the tropics. Part I: Dynamical analysis in the wavenumber-frequency domain. *J Atmos Sci* 37:283-298.
- Zangvil A, Yanai M (1981) Upper tropospheric waves in the tropics. Part II: Association with clouds in the wave number-frequency domain. *J Atmos Sci* 38:939–953.
- Zuluaga MD, Houze Jr RA (2013) Evolution of the population of precipitating convective systems over the equatorial Indian Ocean in active phases of the Madden-Julian Oscillation. *J Atmos Sci* 70:2713-2725.

Figure Captions

- Figure 1 : Evolution of *La Niña* in the Indo-Pacific region during 2011. Sea surface temperature ($^{\circ}\text{C}$) anomaly is plotted during January [a], April [b], July [c] and October [d] to display the evolution.
- Figure 2 : Map of Sea surface temperature anomaly during October 2011 (positive dipole year) over Tropical Indian Ocean (a). Box1 (82-100E; 0 – 10N), Box2 (82-100E; 0-15S) and Box3 (82-100E; 15-25S) are chosen to demarcate cold water (box2) sandwiched between bifurcated warm water (boxes 1&3) during an Indian Ocean Dipole event. The average temperature anomalies in these boxes are displayed as bar diagram during the ten year period prior to 2011 (a) and the black line denote the Dipole Mode Index (DMI).
- Figure 3 : Profiles of temperature ($^{\circ}\text{C}$) (6 hourly time series; white line) superimposed on lapse rate ($^{\circ}\text{C}/100\text{m}$; shown as positive values) (shaded) [a], Relative Humidity (%) [b], Zonal wind (ms^{-1}) [c] and Meridional wind (ms^{-1}) [d] plotted against altitude. The temperature lapse rate ($^{\circ}\text{C}/100\text{m}$) [shaded] is superimposed over the contours. Launch location is at 80°E and 83°E and the line of separation is highlighted by a bold line in the time series plot. The launching times are 00 GMT, 06 GMT, 12 GMT and 18 GMT from 25th Sept. to 3rd Oct. 2011 at 80°E and from 4th to 10th Oct 2011 at 83°E .
- Figure 4 : Wavelet power spectrum of temperature (a,b,c), relative Humidity(d,e,f), U- wind (g,h,i) and V- wind (j,k,l) at lower (left panel), middle (middle panel) and upper (right panel) troposphere. Thick black contours are the 10% significance (90% confidence level) regions.
- Figure 5 : Profiles of temperature ($^{\circ}\text{C}$) (white line) superimposed on lapse rate ($^{\circ}\text{C}/100\text{m}$); shown as positive values (shaded) [a], Relative Humidity (%) [b], zonal wind (m/s) [c] and meridional Wind (m/s) [d] along the meridional section (5°N to 5°S) at 83°E .
- Figure 6 : Hovmuller (Longitude-time) diagram of 20 to 100 day band pass filtered OLR averaged over 10°S - 5°N for the period 1st September to 31st October 2011.
- Figure 7 : Zonal wave number – frequency diagram of anti-symmetric OLR spectral power divided by a background. Superimposed are the dispersion curves of the equatorial waves (MRG) for the three equivalent depths of 12, 25 and 50 m)
- Figure 8 : Time series (top) and Wavelet power spectrum (bottom) plots of Latent Heat Flux (left panel) and Sensible Heat Flux (right panel) using three hourly AWS data collected onboard the ship during the time of the ascend. Thick black contours are the 10% significance (90% confidence level) regions.

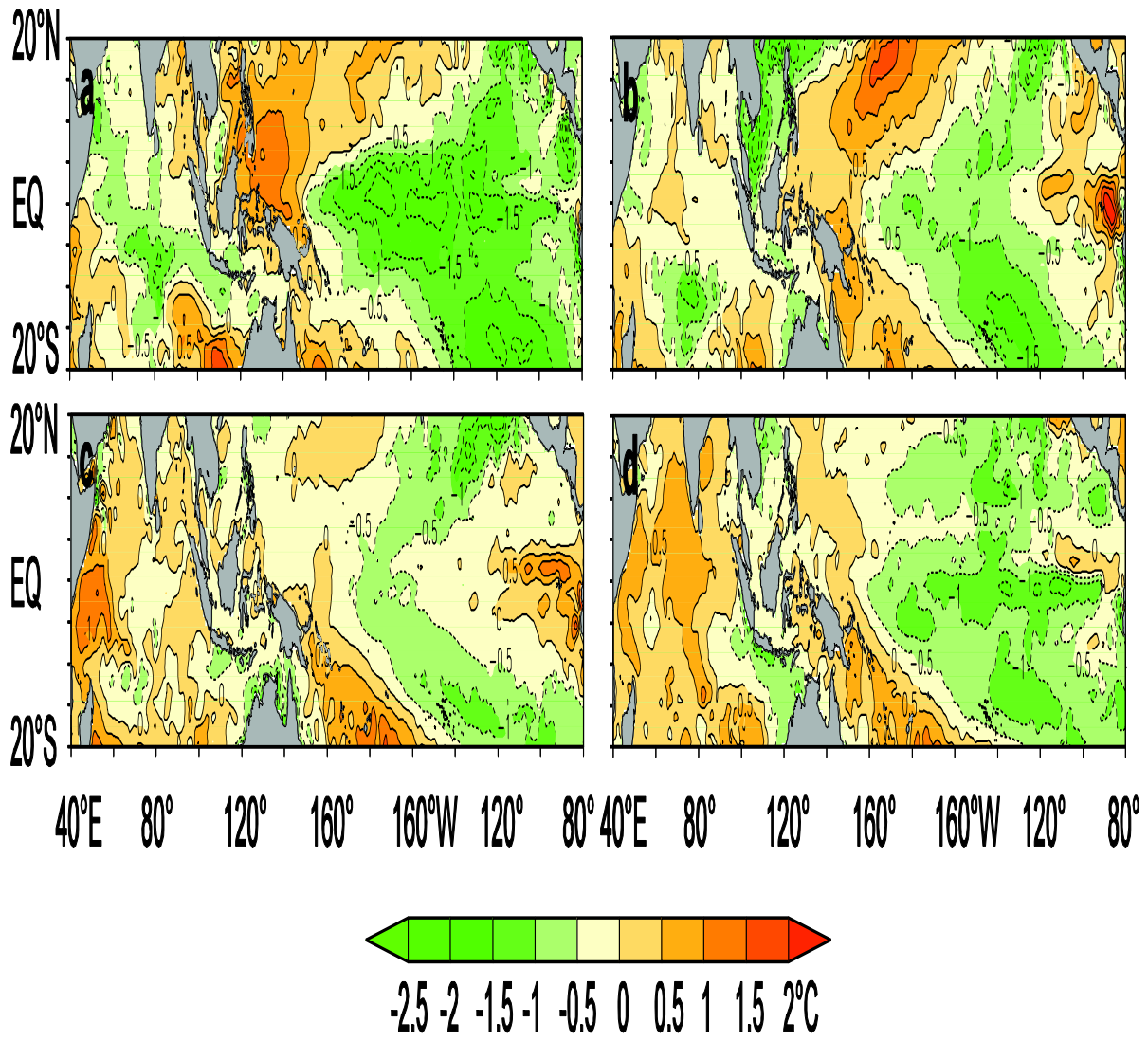


Figure. 1. Evolution of *La Niña* in the Indo-Pacific region during 2011. Sea surface temperature ($^{\circ}\text{C}$) anomaly is plotted during January [a], April [b], July [c] and October [d] to display the evolution.

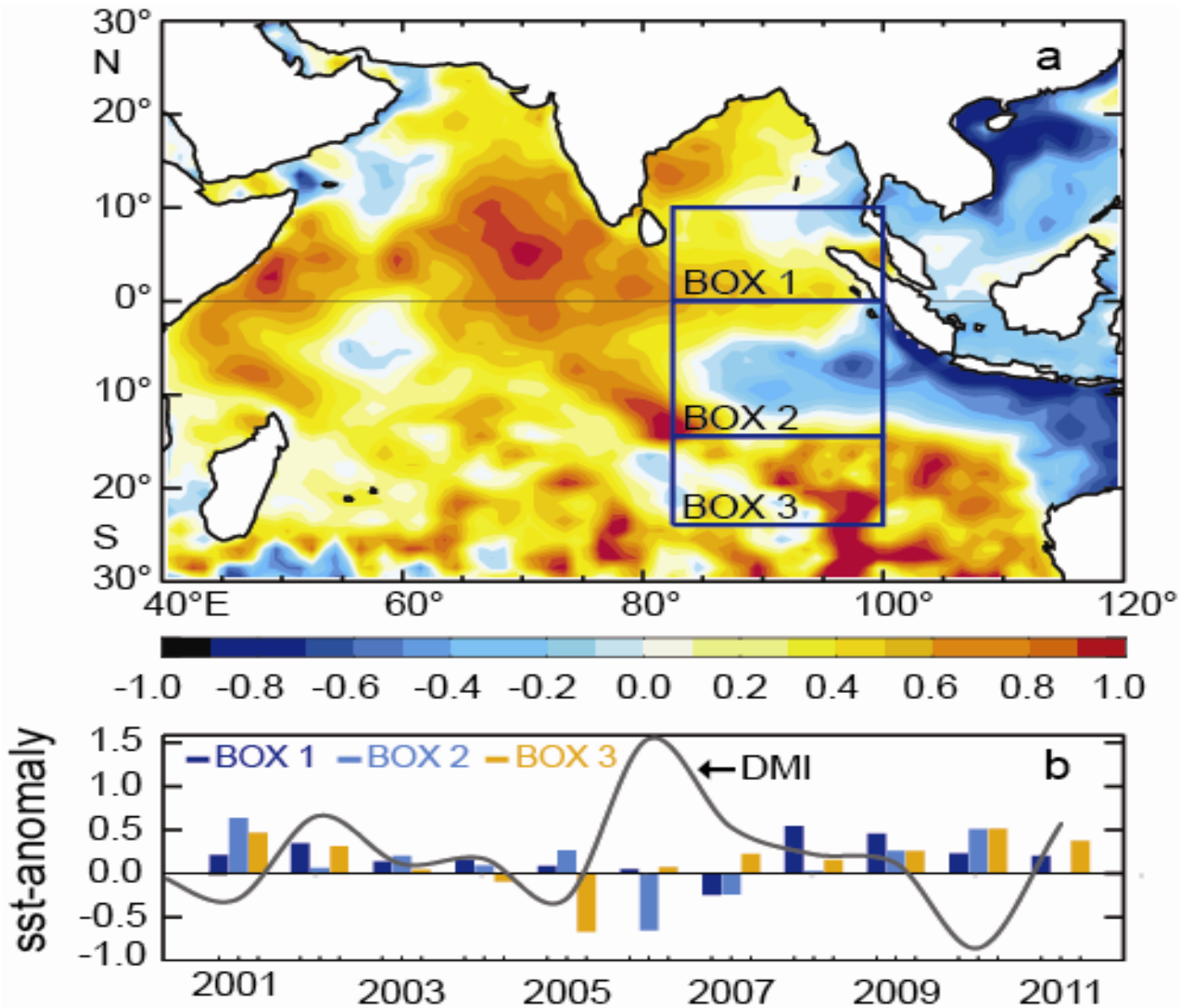


Figure 2. Map of Sea surface temperature anomaly during October 2011 (positive dipole year) over Tropical Indian Ocean (a). Box1 (82-100E; 0 – 10N), Box2 (82-100E; 0-15S) and Box3 (82-100E; 15-25S) are chosen to demarcate cold water (box2) sandwiched between bifurcated warm water (boxes 1&3) during an Indian Ocean Dipole event. The average temperature falling in these boxes are displayed as bar diagram during the ten year period prior to 2011 and the black line denotes the Dipole Mode Index (DMI) (b).

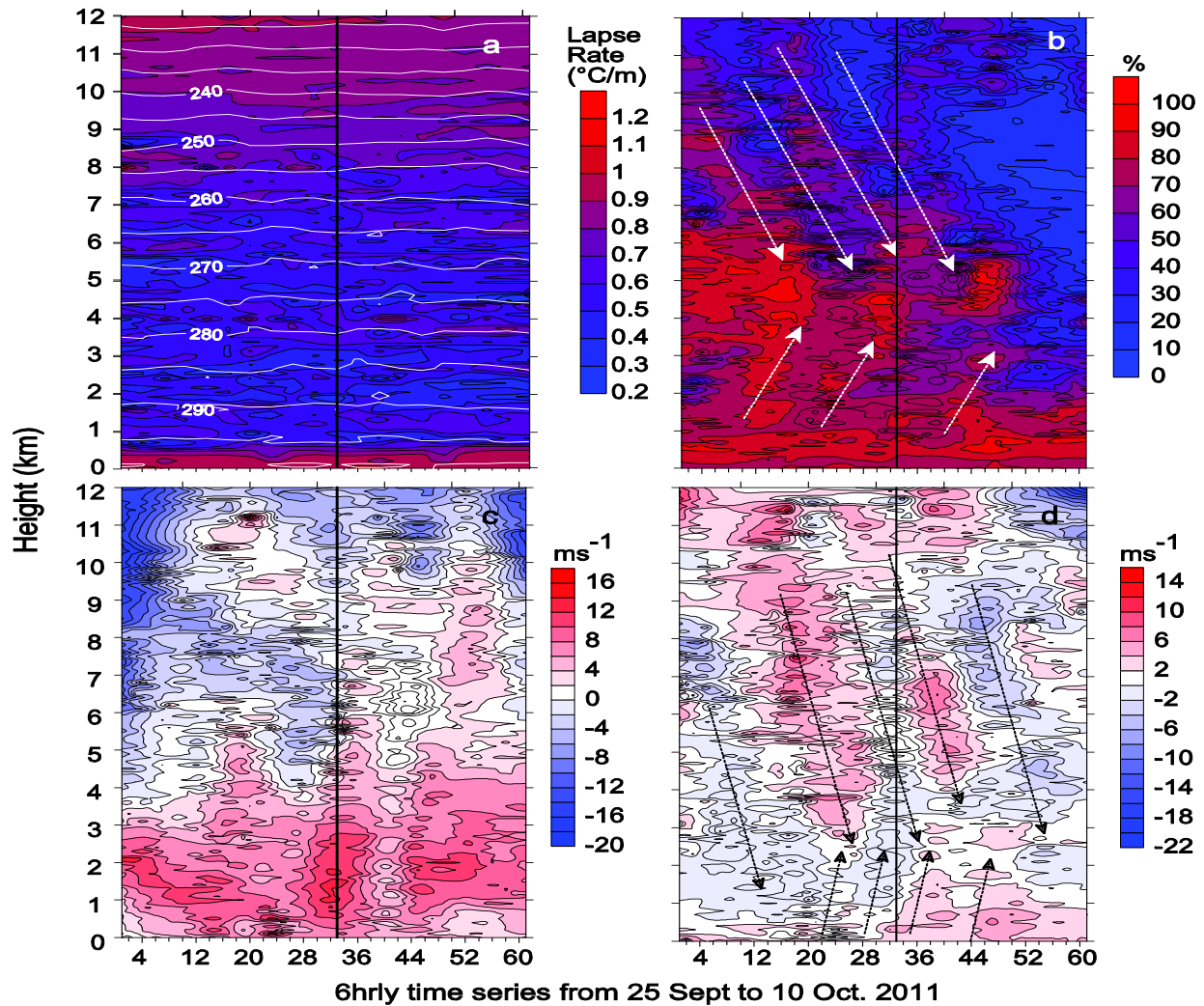


Figure.3. Profiles of temperature ($^{\circ}\text{C}$) (6 hourly time series; white line) superimposed on lapse rate ($^{\circ}\text{C}/\text{m}$) (shaded) [a], Relative Humidity (%) [b], Zonal wind (ms^{-1}) [c] and Meridional wind (ms^{-1}) [d] plotted against altitude. The temperature lapse rate ($^{\circ}\text{C}/\text{m}$) [shaded] is superimposed over the contours. Launch location is at 80°E and 83°E and the line of separation is highlighted by a bold line in the time series plot. The launching times are 00 GMT, 06 GMT, 12 GMT and 18 GMT from 25th Sept. to 3rd Oct. 2011 at 80°E and from 4th to 10th Oct 2011 at 83°E .

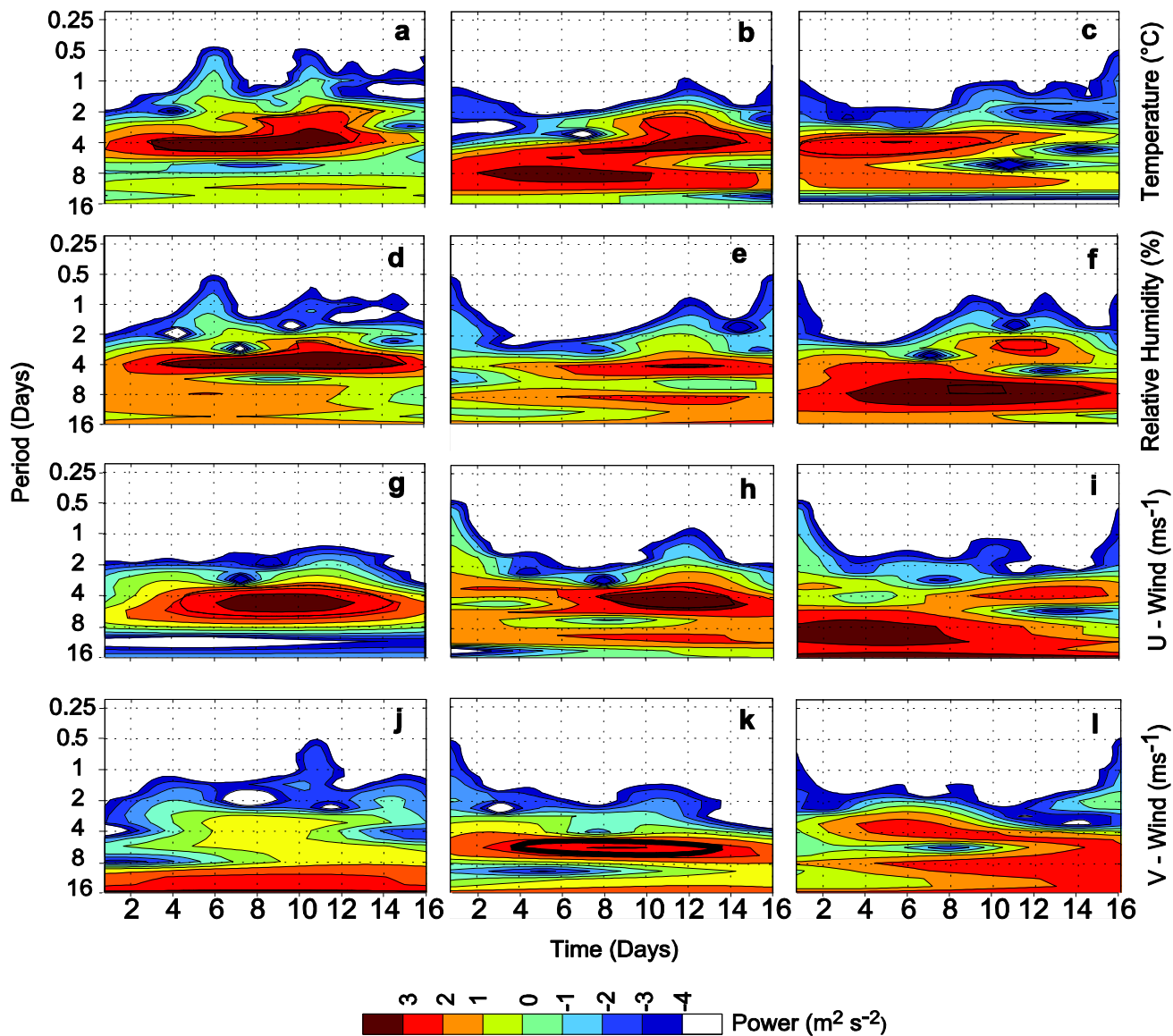


Figure.4. Wavelet power spectrum of temperature (a,b,c), relative Humidity(d,e,f), U- wind (g,h,i) and V- wind (j,k,l) at lower (left panel), middle (middle panel) and upper (right panel) troposphere. Thick black contours are the 10% significance (90% confidence level) regions.

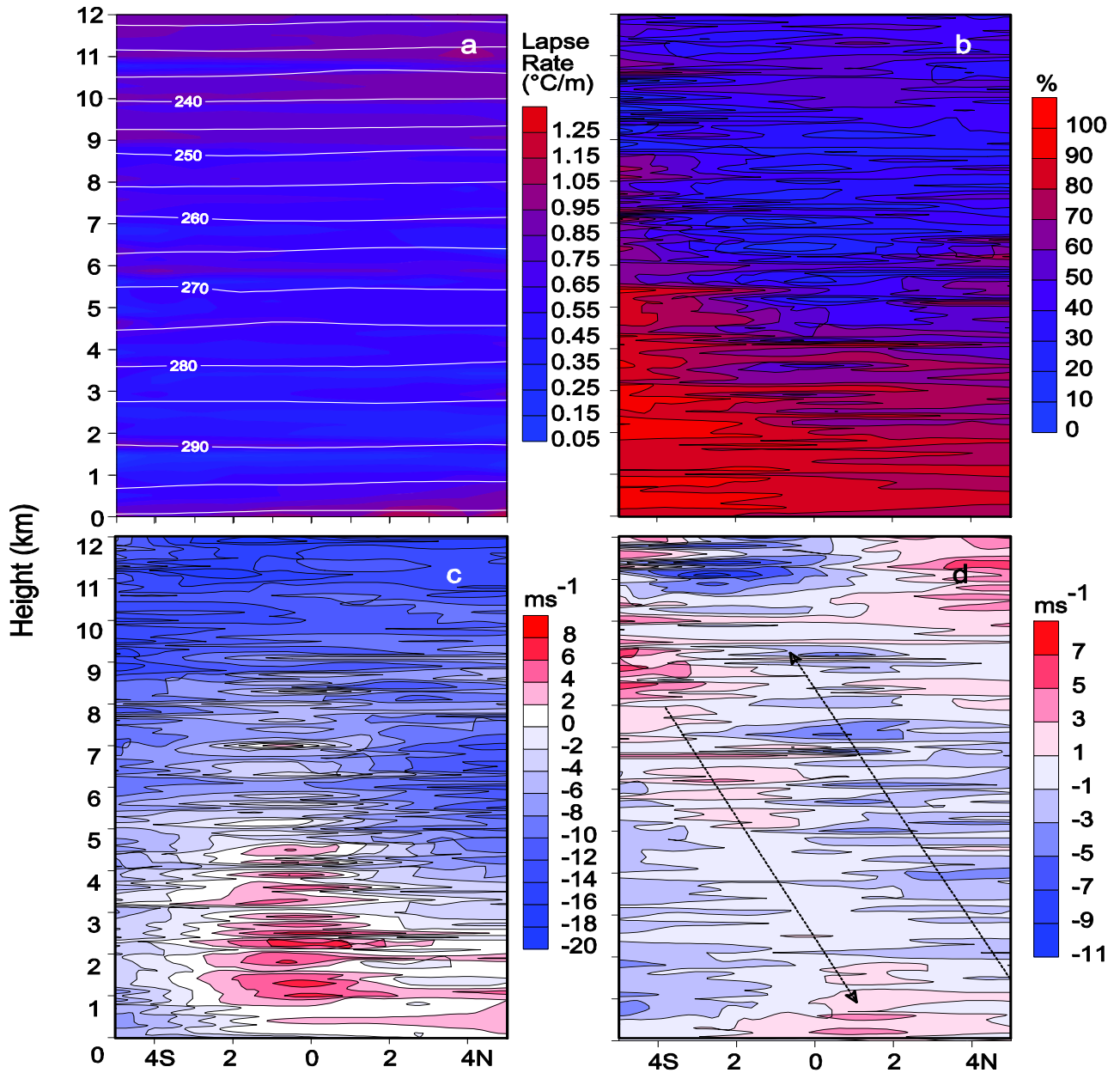


Figure.5.Profiles of temperature ($^{\circ}\text{C}$) (white line) superimposed on lapse rate ($^{\circ}\text{C} / \text{m}$) (shaded) [a], Relative Humidity (%) [b], zonal wind (m/s) [c] and meridional Wind (m/s) [d] along the meridional section (5°N to 5°S) at 83°E .

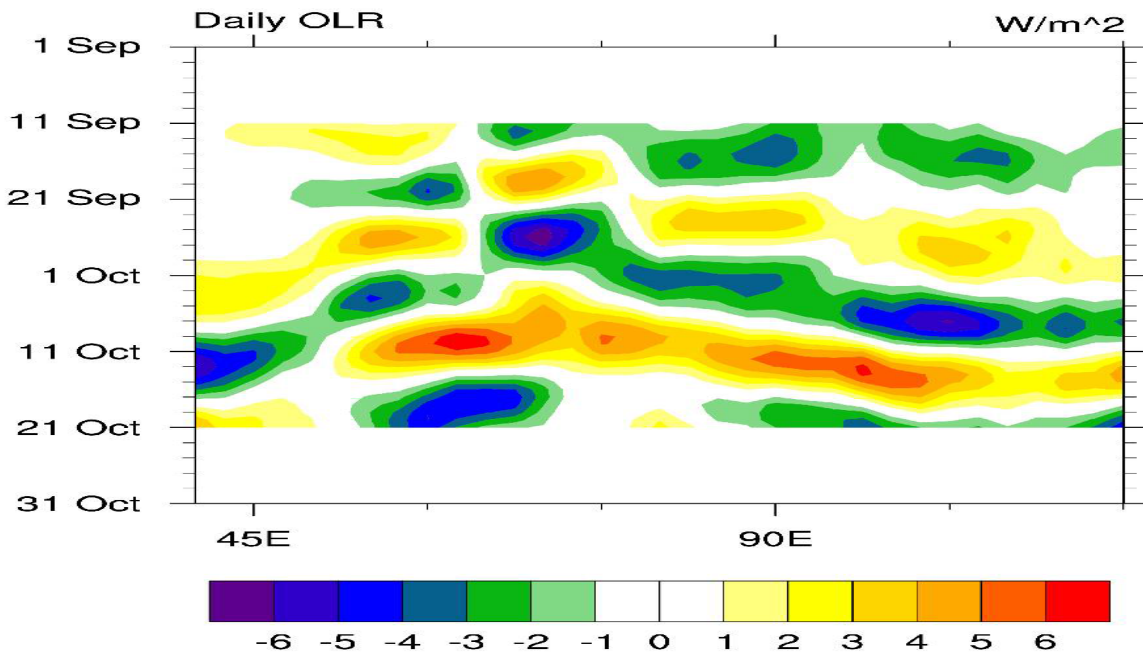


Figure.6.Hovmuller (Longitude-time) diagram of 20 to 100 day band pass filtered OLR averaged over 10⁰ S-5⁰N for the period 1st September to 31st October 2011.

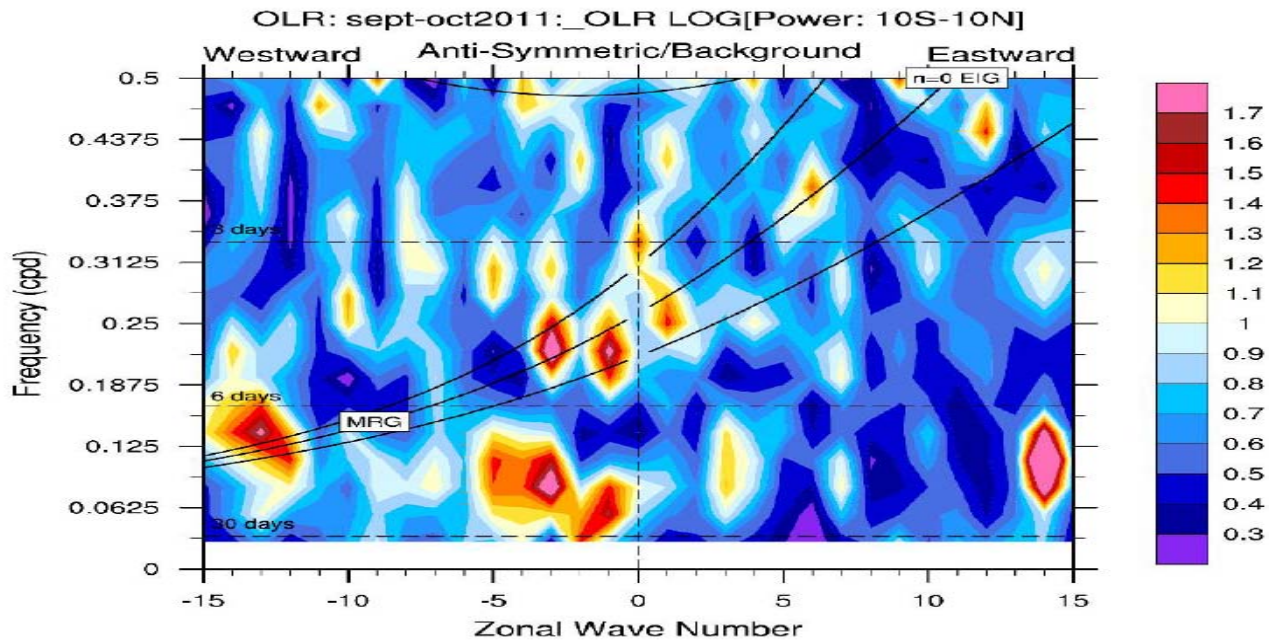


Figure 7. Zonal wave number-frequency diagram of anti-symmetric OLR spectral power divided by a background. Superimposed are the dispersion curves of the equatorial waves (MRG) for the three equivalent depths of 12, 25 and 50 m.

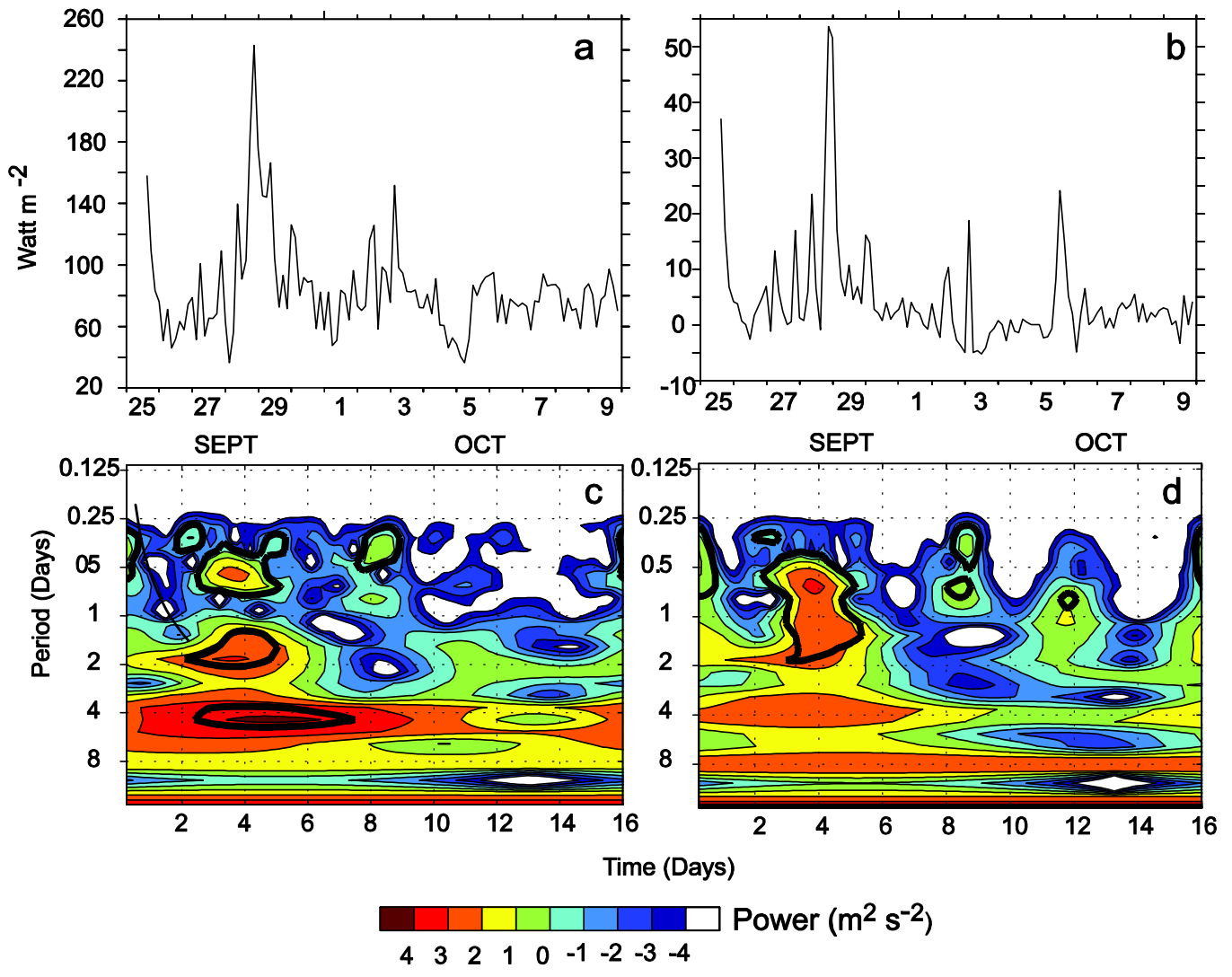


Figure. 8. Time series (top) and Wavelet power spectrum (bottom) plots of Latent Heat Flux (left panel) and Sensible Heat Flux (right panel) using three hourly AWS data collected onboard the ship during the time of the ascend. Thick black contours are the 10% significance (90% confidence level) regions.